Electrochemical Analysis of PVA/PANI/Activated Carbon Nanocomposites for Energy Storage

Ali A. Sallal and Sabah A. Salman
Department of Physics, University of Diyala, 32001 Baqubah, Iraq
alisallal134@gmail.com, pro.dr_sabahanwer@yahoo.com

Keywords: Activated Carbon, Composite Materials, Polyaniline, Orange Peel, Supercapacitor, Electrochemical Properties, Cyclic Voltammetry, Galvanostatic Charge-Discharge.

Abstract: The main objective of this study was to investigate the electrochemical performance of polyaniline (PANI) integrated with activated carbon (AC) derived from orange peels. The core goal was to develop a low-cost, energy-storing material from agricultural waste. Activated carbon was incorporated to enhance the pseudocapacitance and cycle stability of PANI. XRD analysis showed PANI as a highly crystalline material, while AC exhibited broad peaks, indicating a semicrystalline and highly amorphous nature. Raman spectroscopy confirmed the successful synthesis of PANI (evidenced by active quinonoid and polaron structures, specifically the 1589 cm^{-1} band). AC displayed prominent D and G bands, confirming its amorphous, defective structure with an underlying graphitic system (suggested by the ID/IG ratio). Composite materials (CMs) were synthesized using porous AC obtained from carbonized orange peels and PANI. A symmetric supercapacitor cell was fabricated using PVA/PANI/AC nanocomposite films as the electrode, and its electrochemical performance was evaluated using cyclic voltammetry (CV) and galvanostatic charge-discharge (GCD) techniques. The CV curves of the PVA/PANI/AC nanocomposite film showed clearly defined anodic and cathodic peaks, demonstrating excellent redox activity critical for energy storage applications. Crucially, the addition of AC significantly increased the current density and the area under the CV curve compared to the pure PVA film, pointing to a substantial improvement in charge storage capacity. The PVA/PANI/AC nanocomposite achieved a maximum specific capacitance of 80.50 F/g (for sample PPC4), which is notably higher than that of the pure PVA film (55.59 F/g). In conclusion, the successful integration of PANI and AC within a PVA matrix created a composite material that benefits from the polymer's high faradic activity and AC's strong contribution to charge storage. Furthermore, the porous structure enhances ion transport dynamics, positioning this low-cost, waste-derived material as highly promising for supercapacitor applications.

1 INTRODUCTION

Conductive nanostructured polyaniline (PANI) is synthesized through the oxidative chemical polymerization of aniline, utilizing a combination of ammonium persulfate $(NH_4)_2S_2O_8$ and hydrochloric acid (HCl) in an aqueous system. The synthesis is conducted either at 0−5°°C for improved polymerization efficiency [1], a method that negates the need for post-polymerization processing like dialysis to preserve the PANI nanofibers [2], or at ambient temperature [2]. A major limitation of PANI nanofibers is their poor solubility in most common solvents, particularly aqueous solutions. To mitigate this issue without sacrificing PANI core properties [3], various efforts have centered on incorporating stabilizers, such as polyvinyl alcohol (PVA), polymethyl methacrylate (PMMA), and surfactants, to form soluble composites [4]. However, the resulting materials often show poor suitability for film-forming applications. Interestingly, the incorporation of surfactants provides a dual benefit by enhancing both solubility and the electrical conductivity of PANI films [1], [5]. This makes them valuable for PANI composites used in electrical, electronic, and antistatic fields [6]-[8], though the systematic study necessary for a deeper understanding of their electrical properties has yet to be performed.

Activated carbons are mostly used in commercial supercapacitors as electrode material because of their good electrochemical stability, high surface area,

electrochemical properties, etc. As the application of AC is increasing day by day, the large-scale production of AC is hindered by increasing raw material cost and less availability of precursors. However, fossil fuels do not meet this demand as they are not renewable in nature. Hence, utilization of bio-waste as precursor for production of AC can fulfil the demand because of their low-cost accessibility [9].

The structure of AC differs from that of graphite in terms of the distance between layers. The interlayer spacing is 0.34 to 0.35 nm in AC, while it is 0.33 nm in graphite. ACs are divided into graphitizing and non-graphitizing varieties based on their ability to form graphite. There are several graphene layers in the graphitizing carbon that are positioned parallel to one another. Because of the weak cross-linking between the nearby microcrystallites and the underdeveloped porous structure, the carbon produced is sensitive. The strong cross-linking between crystallites makes the non-graphitizing carbons tough, and they exhibit a well-developed microporous structure [10]. The manufacturing of biomass waste-derived ACs could boost economic returns and lower pollution because wood processing, carpentry, and other associated industries have huge raw material supply potential. Kwiatkowski et al. investigated the production of ACs from numerous biomass-derived resources by activation with KOH [10].

Existing research on conductive PANI composites reveals several areas where data are incomplete. For instance, Tetsuo et al. synthesized PANI composites with water-soluble polymers and anionic surfactants [9], but failed to examine how PANI content influences conductivity. Similarly, Amarnath and Palaniappan [3] created PVA-based PANI composites using the low-cost stabilizer gum acacia, resulting in low conductivity (10^{-5}-10^{-4} S/cm), yet they omitted any assessment of component compatibility. The primary focus of studies on these composites generally lies in their electroactive features [10], dc/ac electrical transport [11], [12], and dielectric response [13]. Preparation methods for PVA/nanostructured PANI composites have involved either simply dissolving PANI into PVA [14] or introducing aldehydes to build a semi-interpenetrating network [15] for enhanced properties. Successful alternative routes also include the in situ polymerization of aniline in the presence of PVA [8], [16].

Highly mature electronic components do not meet the increasing demand for biocompatible devices, as their stiff nature contrasts sharply with human tissues. Addressing this issue requires innovative research. Here, we present a new method for creating flexible and customizable hydrogel-based supercapacitors. Wearable technology requires power from both energy harvesting [17] and storage mechanisms [18, 19]. Since harvested energy is sporadic, high-capacity devices must store this power—whether generated internally or supplied externally—using batteries or supercapacitors. Supercapacitors (SCs) are electrochemical storage units capable of fast, high-power energy release [20], [21]. They are primarily divided into two categories: pseudocapacitors, which store energy through redox reactions, and electric double-layer capacitors (EDLCs), which accumulate charge electrostatically at the electrode-electrolyte boundary [22]. SCs are now essential components in consumer and industrial energy systems [21]. The main objective of this paper is to study the Electrochemical process of polyaniline in the activated carbon obtained from the orange peel. Its goal is to obtain a low cost activated carbon able to store energy from agricultural waste.

2 MATERIALS AND METHODS

2.1 Preparation of Polyaniline (PANI)

The preparation starts by pre-cooling 3 mL of distilled aniline in a 50 mL beaker, submerged in an ice bath to maintain a 0◦C temperature for 10 min. Following this, 20 mL of 1M HCl is added slowly. The oxidant, 2 g of Ammonium Persulfate (APS), is first dissolved in another 20 mL of 1M HCl and subsequently introduced dropwise to the aniline solution, while rigorously controlling the temperature at 0°C. The reaction mixture is then stirred under chilling conditions for 2 hr and subsequently stored in a refrigerator overnight to ensure complete polymerization. The solid product is isolated through filtration and subjected to four washes with distilled water. To de-dope the polymer, the precipitate is stirred in 20 mL of 1M ammonium hydroxide (NH_4OH) for 30 min and washed with distilled water again until the washings are pH neutral. For final purification, the solid is washed with 15 mL of benzene, stirred for 15 min, and then dried in an oven at 80◦C for 6 hr.

2.2 Preparation Activated Carbon (AC)

To prepare the activated carbon AC, orange peels were first washed with distilled water and then

pyrolyzed in an oven at 200°C for 2 hr. Following a one-hour cooling period at room temperature, the peels were pulverized. The powder was then chemically activated by soaking it in H_2SO_4 (98%) for 24 hr. Neutralization was carried out by mixing the material with distilled water and $NaHCO_3$ (2:1) for another 24 hr. The mixture was subsequently washed repeatedly with distilled water until a pH of 7 was reached. Finally, the neutralized material was dried in an oven at 110°C for 5 hr to yield the AC product.

2.3 Preparation Nanocomposite Films

A polyvinyl alcohol (PVA) stock solution is initially prepared by dissolving 25 gm of PVA in 250 mL of distilled water. This solution is stirred at 70°C, followed by overnight stirring at room temperature. Next, 10 mL of the PVA stock solution is taken, and a specific quantity of polyaniline (PANI) is dispersed in it, followed by 1hr of magnetic stirring. Different weight ratios (0, 1, 5, 9, and 13 wt%) of the reinforcing materials are then added. The resulting solutions are cast onto clean, dust-free Petri dishes placed on a level surface and left to dry. Once the films are dry, they are carefully detached from the glass and kept in insulated plastic containers until analysis. Finally, the film thickness is determined using a micrometer were 65 µm, with multiple measurements taken across the film's surface for accuracy. The prepared specimens are identified as outlined in Table 1.

Table 1: Sample symbol.

Samples	Symbol
PVA	P
PVA/PANI	PP
PVA/PANI/AC 1 wt %	PPC1
PVA/PANI/AC 5 wt %	PPC2
PVA/PANI/AC 9 wt %	PPC3
PVA/PANI/AC 13 wt %	PPC4

3 RESULT AND DISCUSSION

3.1 X-ray Diffraction (XRD) Analysis

The synthesized polyaniline (PANI) powder and activated carbon (AC) were characterized using X-ray diffraction (XRD), as shown in Figure 1. The XRD spectrum (Fig. 1a) confirms the crystalline structure of the PANI nanofibers. The pattern is marked by three sharp diffraction peaks around 15.6°, 20.7°, and 25.5° (2θ). These peaks correspond to the (121), (113), and (322) planes, representing scattering perpendicular and parallel to the polymer chain [23], [24], and are consistent with JCPDS card no. 72-0634. The notable intensification of the major peak suggests an enlargement of the powder's crystallite size [25]. The observed partial crystallinity is thought to stem from the strong intermolecular and intramolecular hydrogen bonding facilitated by the amine and imine groups within the doped PANI [26]. Overall, the distinct peaks confirm that the PANI synthesized is highly crystalline [23].

Figure 1b presents the XRD pattern obtained for the AC specimen. This pattern is defined by broad peaks centered at 2θ values of 25.09° and 43.85°. These diffraction signals can be assigned to the (002) and (100) Miller indices, respectively, which align well with the reference standard JCPDS card no. 041-1487 [27]. The presence of these wide peaks is characteristic of a turbostratic structure—a form of graphite where the layers are significantly disordered. Consequently, the AC possesses an intermediate structure that falls between completely amorphous carbon and perfectly ordered graphite [27]. The overall broadness of the peaks serves as confirmation of the highly amorphous nature of the prepared carbon [28]. This partial crystallinity is crucial as it creates pathways for electron transport, enhancing conductivity, while the highly disordered, amorphous regions contribute to structural integrity, increasing mechanical strength and elasticity.

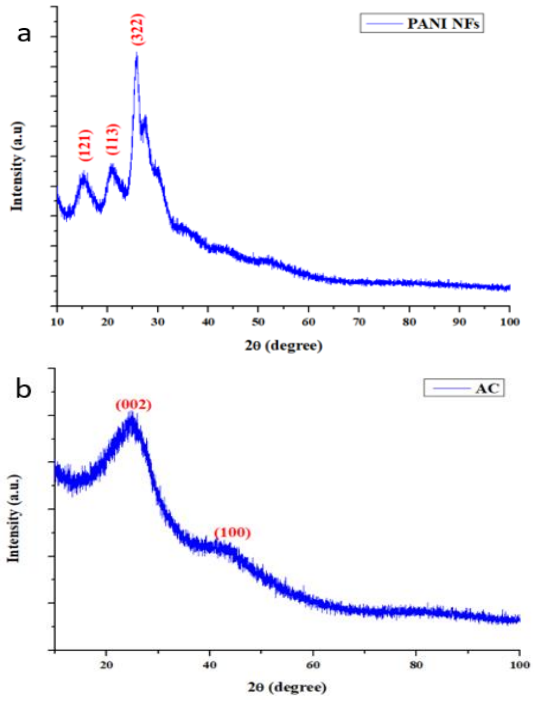

Figure 1: XRD of (a) PANI NFs (b) Activated carbon (AC).

The 2θ values for prominent peaks, corresponding (*hkl*) are represented in Table 2.

Table 2: XRD analysis of PANI and AC.

Pawder	2θ	(*hkl*) plane
PANI	15.6	121
	20.7	113
	25.5	322
AC	25.09	100
	43.85	002

3.2 Raman Analysis

Figure 2a, b displays the laser Raman spectra for the individual polyaniline (PANI) and activated carbon (AC) powders. Raman spectroscopy is an exceptionally effective method for determining a material's molecular composition.

The PANI Raman spectrum (Fig. 2a) reveals several characteristic bands, located approximately at 1589, 1503, 1412, 1336, 1236, and 1167 cm^{-1}, which confirm the presence of PANI's organic components. Specifically, the strong signal near 1589 cm^{-1} is assigned to the C=N stretching vibrations within the quinoid structure. The peak at 1503 cm^{-1} corresponds to the C=C stretching deformation of the benzenoid rings. The band observed at 1336 cm^{-1} is a characteristic C-N stretching mode in the benzenoid structure. Furthermore, the peak at 1167 cm^{-1} indicates aromatic C-H in-plane bending. The signal at 1236 cm^{-1} is associated with the C-N^{+} stretching and vibrational modes of PANI's polaron structure. Finally, the feature near 901 cm^{-1} is attributed to C=H out-of-plane flexure in the benzene rings, providing further evidence of successful PANI synthesis during the polymerization process [29].

The Raman spectrum of the AC sample is depicted in Figure 2b. The material exhibits two significant signals: the G-band at approximately 1604 cm^{-1} and the D-band at 1357 cm^{-1}. These bands correspond to the ordered graphitic structure and the disordered carbon (defects), respectively. The imperfections observed in the spectrum confirm that the sample is built upon an sp^2 carbon framework, composed of either C=C chains or aromatic ring systems. The wide spectral peaks confirm the amorphous nature of the carbon. Although amorphous, the calculated intensity ratio of ID/IG is 1.18, It is calculated by dividing the height of peak D by the height of peak G after the matching process. This method is simpler but may be less accurate for wide, overlapping peaks, suggesting the co-existence of an underlying ordered carbon arrangement [28]. This structural information, derived from the Raman spectrum, is key to understanding the charge storage mechanisms and predicting the electrochemical performance of the resulting nanofilms.

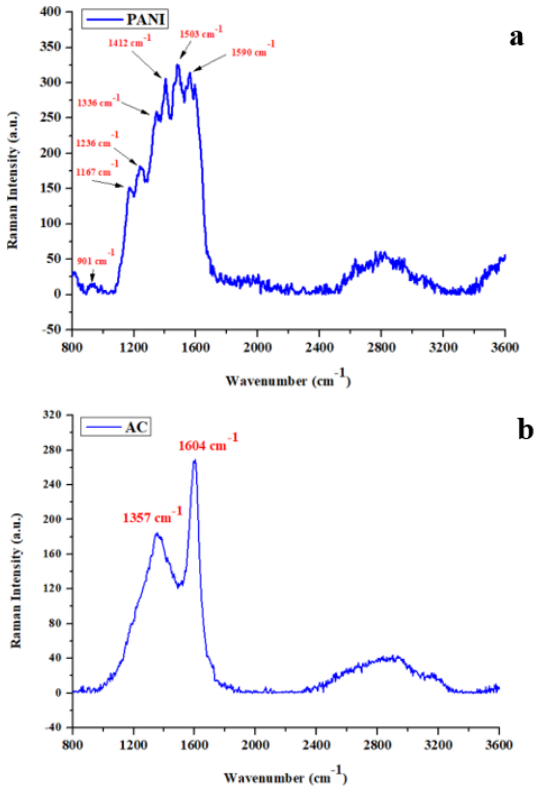

Figure 2: Raman spectra of (a) Polyaniline (PANI) (b) Activated Carbon (AC).

3.3 Electrochemical Properties

Electrochemical characteristics of the composite materials were studied via cyclic voltammetry (CV) in 1 M Na_2SO_4 at ambient temperature. Figure 3 shows the CV curves for PVA/PANI/AC nanocomposite films across Activated carbon (AC) loadings of 1, 5, 9, and 13 wt%.

Introducing polyaniline (PANI) alters the CV curve. Below ~0.2 V, the current decreases as polymer content rises. Since the carbon material primarily governs the response in this low-potential region, this reduction implies PANI is partially insulating the carbon surface [30].

The CV of the PVA sample is nearly identical to the PVA/PANI and PVA/PANI/AC curves. The presence of a poorly defined, wide peak suggests faradaic reactions are occurring. The PPC1 sample shows an increase in intensity for the diffuse peaks at 0.4 V and 0.25 V. Continued increases in PANI concentration lead to the anodic peak becoming

sharper, more pronounced, and shifting to 0.65 V (with the cathodic peak shifting to 0.27 V). Interestingly, any additional increase in polymer content primarily results in a large surge in peak intensity, rather than further potential shifts.

The CV curve for the composite with the highest polymer content (PPC4) is comparable to that of pure PANI. Two notable differences persist: (1) Current intensity is significant between 0.06 V and 0.5 V. This high current is attributed to the carbon material, which displays a strong electrochemical signal in this range [30]. (2) The leucoemeraldine/emeraldine transition is displaced to a more cathodic potential compared to the neat polymer, even at high polymer loadings. This displacement is thought to be the result of the carbon material promoting ion migration, thus expediting the oxidation-reduction processes [30].

Figures 3 clearly show that the cyclic voltammetry (CV) curve for PVA, PANI, and the PVA/PANI/AC composite display well-defined anodic and cathodic peaks, signifying excellent redox activity. Following the compounding with AC, the (PVA/PANI/AC) composite's current density and the CV area are substantially larger than those of pure PVA when measured at an identical sweep speed. The oxidation potentials are located in the 0.5 V to 0.67 V range, and the reduction potentials appear between 0.2 V and 0.3 V. A closer look at the peak structure reveals that the overall shape results from the partial superposition of two sets of oxidation-reduction peaks.

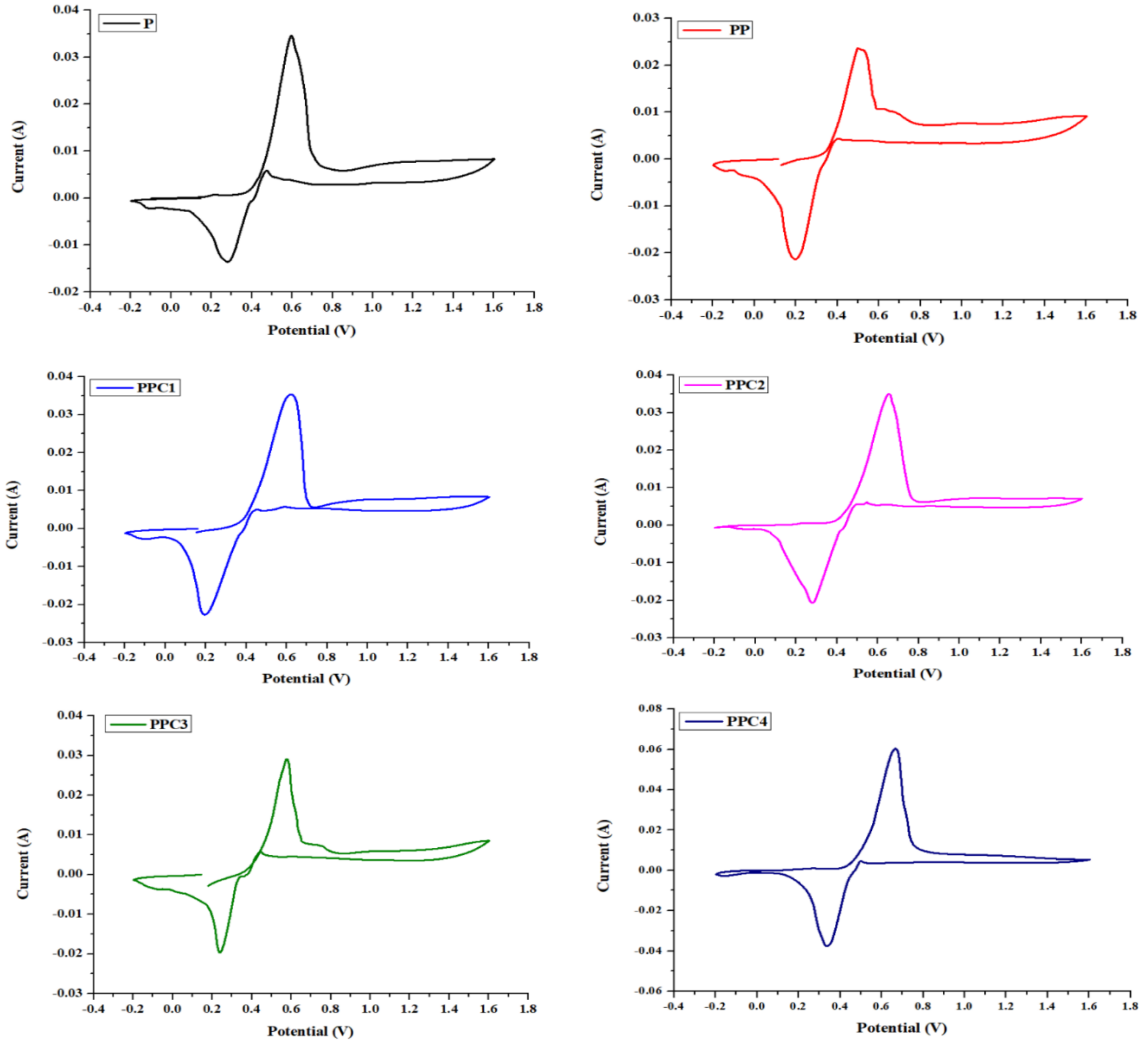

Figure 3: Cyclic voltammogram of PVA, PANI and PVA/PANI/AC nanocomposite. The scan rate is 50 mV/s, electrolyte – 1 M Na_2SO_4.

The capacitive properties of the polyaniline composites described exhibit significant variability. As demonstrated in Figures 4, the specific capacitance values for the PVA/PANI/AC nanocomposite films range from 55.59 to 80.50 F/g through the equation;

$$Cs = \frac{A\,\Delta t}{m\,\Delta V}. \quad \ldots \ldots (1)$$

Where A: Area under curve, m: mass of sample on the electrode surface (mg) equals to (30 mg), ΔV: range of applied potential (V).

The pristine PVA polymer film shows a specific capacitance of 55.59 F/g at a 5 mV/s sweep rate. The correlation between specific capacitance and PANI concentration is contingent on the properties of the AC, the synthesis route, and the electrode fabrication technique.

The maximum capacitance of 80.50 F/g was achieved by the PPC4 sample, which was based on AC, while the PP sample exhibited a substantially lower capacitance of 59.2 F/g [31]. This contrast is typically attributed to the formation of a dense, thick layer during electrochemical electrode preparation, which severely hampers the efficient utilization of the active material [32]. Previous studies suggest that this behavior is caused by the excessive polymer content obstructing the conductive network of the AC, resulting in increased charge-transfer resistance and a corresponding decay in capacitance. Conversely, in the current study, specific capacitance is observed to increase with the amount of AC. This linear relationship strongly suggests the formation of a porous structure that is readily accessible to electrolyte ions, thus facilitating both ion and electron transport [30].

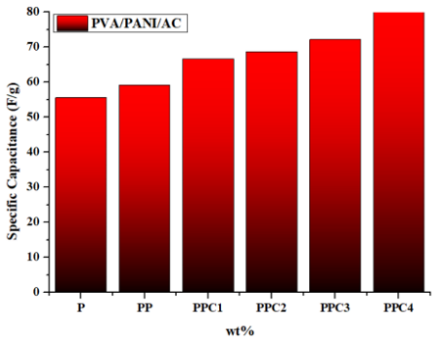

Figure 4: Specific capacitance of PVA, PANI and PVA/PANI/AC nanocomposite films.

Galvanostatic charge-discharge (GCD) experiments were executed on PVA, PANI, and PVA/PANI/AC nanocomposite films at 1 A/g within a potential window of 0 to 1.4 V. The curves exhibit excellent triangular symmetry, affirming the strong capacitive performance of the composites, despite a small observed iR drop. The slight non-linearity in the GCD plots is associated with the redox activity of the electrode constituents [33].

The discharge time, and consequently the specific capacitance, follows the trend: PPC4>PPC3>PPC2>PPC1>PP>P as show in Table 3. This ordering aligns consistently with the cyclic voltammetry results. The data confirms that the composite electrodes possess enhanced specific capacitance stemming from pseudocapacitance, with the PPC4 sample achieving the highest measured specific capacitance, PPC4 has an ideal micropore-to-mesopore ratio, maximizing the total accessible surface area and allowing fast ion diffusion, which translates to high specific capacitance. [33].

Table 3: Value of specific capacitance.

Sample	Specific capacitance (F/g)
P	55.59
PP	59.2
PPC1	66.66
PPC2	68.75
PPC3	72.22
PPC4	80.5

4 CONCLUSIONS

This research definitively demonstrated that the incorporation of activated carbon acts as a potent modifier for polyaniline (PANI). The synergistic effect achieved by combining PANI's inherent high Faradaic activity with the high surface area of the AC led to a superior composite material. Crucially, this collaboration significantly enhanced the material's ability to store charge, evidenced by the dramatically increased specific capacitance observed in the optimized sample (PPC4). This performance enhancement arises from two key mechanisms. Structurally, the activated carbon AC, with its highly developed specific surface area and porous structure, serves as an effective structural backbone. It ensures the uniform dispersion of PANI particles, preventing their aggregation and maximizing the electrochemically active area accessible to the electrolyte, ion Dynamics. The porous nature of the activated carbon facilitates rapid and efficient diffusion of electrolyte ions throughout the entire electrode structure. This enhanced ion transport ensures a more complete and effective utilization of the conductive polymer (PANI), which is essential for

achieving high charge/discharge rates and robust performance. The resulting combination yields a superior capacitive and operational performance, positioning these nanocomposites as highly promising candidates for use as the active electrode component in advanced supercapacitor (SCs) devices. A critical achievement of this work is the use of orange peel-derived AC. This approach not only provides a high-performance material but also offers a sustainable and exceptionally cost-effective pathway for converting agricultural waste into valuable technology.

ACKNOWLEDGMENTS

The authors wish to express their profound gratitude to the Department of Physics, College of Science, University of Diyala, for their consistent support and the essential facilities provided for the execution of this research. Furthermore, appreciation is extended to all colleagues and technical staff whose expert guidance and invaluable assistance were instrumental to the successful completion of this study.

REFERENCES

[1] M. C. Arenas, E. Andablo, and V. M. Castaño, "Synthesis of conducting polyaniline nanofibers from single and binary dopant agents," J. Nanosci. Nanotechnol., vol. 10, no. 1, pp. 549-554, 2010, [Online]. Available: https://doi.org/10.1166/jnn.2010.1691.

[2] P. C. Wang, E. C. Venancio, D. M. Sarno, and S. A. MacDiarmid, "Simplifying the reaction system for the preparation of polyaniline nanofibers: Re-examination of template-free oxidative chemical polymerization of aniline in conventional low-pH acidic aqueous media," React. Funct. Polym., vol. 69, no. 4, pp. 217-223, 2009, [Online]. Available: https://doi.org/10.1016/j.reactfunctpolym.2008.12.012.

[3] A. Fattoum, Z. B. Othman, and M. Arous, "Dc and Ac conductivity of polyaniline/poly (methyl methacrylathe) blends below the percolation threshold," Mater. Chem. Phys., vol. 135, no. 1, pp. 117-122, 2012, [Online]. Available: https://doi.org/10.1016/j.matchemphys.2012.03.078.

[4] S. A. Salman, N. A. Bakr, and S. S. Abduallah, "Study of thermal decomposition and FTIR for PVA-AlCl3 composite films," J. Eng. Appl. Sci., vol. 14, pp. 717-724, 2019.

[5] T. Hino, T. Namiki, and N. Kuramoto, "Synthesis and characterization of novel conducting composites of polyaniline prepared in the presence of sodium dodecylsulfonate and several water soluble polymers," Synth. Met., vol. 156, pp. 1327-1332, 2006, [Online]. Available: https://doi.org/10.1016/j.synthmet.2006.09.006.

[6] M. O. Ansari and F. Mohammad, "Thermal stability and electrical properties of dodecyl-benzene-sulfonic-acid doped nanocomposites of polyaniline and multi-walled carbon nanotubes," Compos. Part B: Eng., vol. 43, no. 8, pp. 3541-3548, 2012, [Online]. Available: https://doi.org/10.1016/j.compositesb.2012.05.009.

[7] L. Chen, H. Ding, G. Zhou, Y. Zhu, and D. Hui, "Preparation, characterization and thermoelectricity of ATT/TiO2/PANI nano-composites doped with different acids," Compos. Part B: Eng., vol. 45, no. 1, pp. 111-116, 2013, [Online]. Available: https://doi.org/10.1016/j.compositesb.2012.09.006.

[8] M. A. Soto-Oviedo, O. A. Araújo, R. Faez, M. C. Rezende, and M. A. De Paoli, "Antistatic coating and electromagnetic shielding properties of a hybrid material based on polyaniline/organoclay nanocomposite and EPDM rubber," Synth. Met., vol. 156, no. 18-20, pp. 1249-1255, 2006, [Online]. Available: https://doi.org/10.1016/j.synthmet.2006.09.002.

[9] M. Dhelipan, A. Arunchander, A. K. Sahu, and D. Kalpana, "Activated carbon from orange peels as supercapacitor electrode and catalyst support for oxygen reduction reaction in proton exchange membrane fuel cell," J. Saudi Chem. Soc., vol. 21, no. 4, pp. 487-494, 2017, [Online]. Available: https://doi.org/10.1016/j.jscs.2014.07.001.

[10] J. L. Figueiredo, C. A. Bernardo, R. T. K. Baker, and K. J. Hüttinger, Carbon fibers filaments and composites, vol. 177, Springer Science & Business Media, 2013, [Online]. Available: https://doi.org/10.1007/978-94-017-0624-9.

[11] Y. Yang, S. Chen, and L. Xu, "Enhanced conductivity of polyaniline by conjugated crosslinking," Macromol. Rapid Commun., vol. 32, no. 7, pp. 593-597, 2011, [Online]. Available: https://doi.org/10.1002/marc.201000676.

[12] A. Mirmohseni and G. G. Wallace, "Preparation and characterization of processable electroactive polyaniline–polyvinyl alcohol composite," Polymer, vol. 44, no. 12, pp. 3523-3528, 2003, [Online]. Available: https://doi.org/10.1016/S0032-3861(03)00276-8.

[13] A. Fattoum, Z. B. Othman, and M. Arous, "Dc and Ac conductivity of polyaniline/poly (methyl methacrylathe) blends below the percolation threshold," Mater. Chem. Phys., vol. 135, no. 1, pp. 117-122, 2012.

[14] P. Utta, M. Biswas, M. Ghosh, S. K. De, and S. Chatterjee, "The dc and ac conductivity of polyaniline–polyvinyl alcohol blends," Synth. Met., vol. 122, no. 2, pp. 455-461, 2001, [Online]. Available: https://doi.org/10.1016/S0379-6779(01)00302-3.

[15] M. Das, A. Akbar, and D. Sarkar, "Investigation on dielectric properties of polyaniline (PANI) sulphonic acid (SA) composites prepared by interfacial polymerization," Synth. Met., vol. 249, pp. 69-80, 2019, [Online]. Available: https://doi.org/10.1016/j.synthmet.2019.01.011.

[16] M. F. Banjar et al., "Synthesis and characterization of a novel nanosized polyaniline," Polymers, vol. 15, no. 23, p. 4565, 2023, [Online]. Available: https://doi.org/10.3390/polym15234565.

[17] X. Yu et al., "Self-assembly of flower-like polyaniline–polyvinyl alcohol multidimensional architectures from 2D petals," Mater. Lett., vol. 65, no. 17-18, pp. 2812-2815, 2011, [Online]. Available: https://doi.org/10.1016/j.matlet.2011.06.009.

[18] Y. Kaykha and M. Rafizadeh, "Template synthesis of fibrillar polyaniline complex using a degradable polyelectrolyte," Mater. Chem. Phys., vol. 229, pp. 98-105, 2019, [Online]. Available: https://doi.org/10.1016/j.matchemphys.2019.03.056.

[19] M. N. Hasan, S. Sahlan, K. Osman, and M. S. Mohamed Ali, "Energy harvesters for wearable electronics and biomedical devices," Adv. Mater. Technol., vol. 6, no. 3, 2021, [Online]. Available: https://doi.org/10.1002/admt.202000858.

[20] Z. Liu et al., "Advances in flexible and wearable energy-storage textiles," Small Methods, vol. 2, no. 11, 2018, [Online]. Available: https://doi.org/10.1002/smtd.201800204.

[21] C. Y. Chan et al., "Recent advances of hydrogel electrolytes in flexible energy storage devices," J. Mater. Chem. A, vol. 9, no. 4, pp. 2043-2069, 2021, [Online]. Available: https://doi.org/10.1039/D0TA11451K.

[22] K. Keum et al., "Flexible/stretchable supercapacitors with novel functionality for wearable electronics," Adv. Mater., vol. 32, no. 51, 2020, [Online]. Available: https://doi.org/10.1002/adma.202003180.

[23] K. Keum et al., "Flexible/stretchable supercapacitors with novel functionality for wearable electronics," Adv. Mater., vol. 32, no. 5, 2020.

[24] D. Govindarajan and K. K. Chinnakutti, "Fundamentals, basic components and performance evaluation of energy storage and conversion devices," in Oxide Free Nanomaterials for Energy Storage and Conversion Applications, Elsevier, 2022, pp. 51-74, [Online]. Available: https://doi.org/10.1016/B978-0-323-90956-6.00003-8.

[25] G. V. Ramana et al., "Electrochemically active polyaniline (PANi) coated carbon nanopipes and PANi nanofibers containing composite," J. Nanosci. Nanotechnol., vol. 15, no. 2, pp. 1338-1343, 2015, [Online]. Available: https://doi.org/10.1166/jnn.2015.9189.

[26] Z. H. Mahmoud et al., "Polyaniline/TiO2 nanocomposite for high performance supercapacitor," Bull. Chem. Soc. Ethiopia, vol. 38, no. 4, pp. 1177-1188, 2024, [Online]. Available: https://doi.org/10.4314/bcse.v38i4.17.

[27] S. A. Hasoon and S. A. Abdul-Hadi, "Chemical Synthesis and Characterization of Conducting Polyaniline," Baghdad Sci. J., vol. 17, no. 1, pp. 106-111, 2020, [Online]. Available: https://doi.org/10.21123/bsj.2020.17.1.0106.

[28] S. Najim and A. J. Salim, "Polyaniline nanofibers and nanocomposites: Preparation, characterization, and application for Cr (VI) and phosphate ions removal from aqueous solution," Arabian J. Chem., vol. 10, pp. S3459-S3467, 2017, [Online]. Available: https://doi.org/10.1016/j.arabjc.2013.11.019.

[29] L. A. de Sousa Ribeiro, L. A. Rodrigues, and G. P. Thim, "Preparation of activated carbon from orange peel and its application for phenol removal," Int. J. Eng. Res. Sci., vol. 3, pp. 2395-6992, 2017.

[30] M. Tomy, M. A. Anu, T. V. Anitha, T. V. Vimalkumar, and T. S. Xavier, "Polyaniline-modified renewable coconut husk-derived activated carbon as an efficient electrode for supercapacitor applications-A sustainable approach," Materials Science and Engineering: B, vol. 321, p. 118456, 2025, [Online]. Available: https://doi.org/10.1016/j.mseb.2025.118456.

[31] M. Boutahir et al., "Raman analysis of graphene/PANI nanocomposites for photovoltaic," in International Conference on Advanced Intelligent Systems for Sustainable Development, Cham: Springer International Publishing, vol. 912, pp. 158-163, 2018, [Online]. Available: https://doi.org/10.1007/978-3-030-01997-6_17.

[32] M. V. Lebedeva et al., "Rice husk derived activated carbon/polyaniline composites as active materials for supercapacitors," Int. J. Electrochem. Sci., vol. 13, no. 4, pp. 3674-3690, 2018, [Online]. Available: https://doi.org/10.20964/2018.04.53.

[33] L. L. Zhang et al., "Enhancement of electrochemical performance of macroporous carbon by surface coating of polyaniline," Chem. Mater., vol. 22, no. 3, pp. 1195-1202, 2010, [Online]. Available: https://doi.org/10.1021/cm9029329.